ORIGINAL ARTICLE

Mitochondrial dysfunction underlies cognitive defects as a result of neural stem cell depletion and impaired neurogenesis

Mireille Khacho, Alysen Clark, Devon S. Svoboda, Jason G. MacLaurin, Diane C. Lagace, David S. Park and Ruth S. Slack*

Department of Cellular and Molecular Medicine, University of Ottawa Brain and Mind Research Institute, Ottawa, ON K1H 8M5, Canada

*To whom correspondence should be addressed at: Department of Cellular and Molecular Medicine, Faculty of Medicine, University of Ottawa, 451 Smyth Road, Ottawa, ON K1H 8M5, Canada. Tel: +16135625800 ext. 8458; Email: rslack@uottawa.ca

Abstract

Mitochondrial dysfunction is a common feature of many genetic disorders that target the brain and cognition. However, the exact role these organelles play in the etiology of such disorders is not understood. Here, we show that mitochondrial dysfunction impairs brain development, depletes the adult neural stem cell (NSC) pool and impacts embryonic and adult neurogenesis. Using deletion of the mitochondrial oxidoreductase AIF as a genetic model of mitochondrial and neurodegenerative diseases revealed the importance of mitochondria in multiple steps of the neurogenic process. Developmentally, impaired mitochondrial function causes defects in NSC self-renewal, neural progenitor cell proliferation and cell cycle exit, as well as neuronal differentiation. Sustained mitochondrial dysfunction into adulthood leads to NSC depletion, loss of adult neurogenesis and manifests as a decline in brain function and cognitive impairment. These data demonstrate that mitochondrial dysfunction, as observed in genetic mitochondrial and neurodegenerative diseases, underlies the decline of brain function and cognition due to impaired stem cell maintenance and neurogenesis.

Introduction

During aging and in certain genetic and neurodegenerative diseases, such as Parkinson's, Alzheimer's and Dominant Optic Atrophy, mitochondria become fragmented and their metabolism declines, leading to a progressive loss of function (1,2). Given the vulnerability of neurons to bioenergetic fluctuations, it is not surprising that defects in mitochondrial function would contribute to the neuronal death observed in neurodegenerative diseases (3). In fact, the neurological dysfunctions associated with such diseases have been generally attributed to the resultant loss of post-mitotic neurons, given the high-energy demanding nature of these cells. Recently, our studies and others have revealed an important role for mitochondria in stem cell

regulation (4–7). Thus a question that arises is whether mitochondrial dysfunction, as observed in genetic diseases targeting brain function, may also impact the generation of neurons during development and adulthood.

The fundamental basis of brain development begins with the differentiation of neural progenitor cells (NPCs) into neurons. This process, referred to as neurogenesis, consists of a complex series of events that rely on intricately regulated molecular signaling pathways. Defects or impairments in embryonic neurogenesis have been shown to contribute to many neurodevelopmental disorders and neuropsychiatric diseases (8,9). Neurogenesis is an ongoing process, not solely restricted during brain development, but continuing throughout

adulthood in the subventricular zone (SVZ) and the dentate gyrus (DG) of the hippocampus (10–13). Since the discovery of adult neurogenesis numerous studies have established the functional significance of adult neurogenesis, particularly in the DG. Extensive evidence now reveals that the generation and integration of newborn neurons into the DG of the adult hippocampus play a critical role in cognitive function (14,15), such as learning and memory (13,16). For example, there is compelling evidence that adult neurogenesis is important in hippocampal function and the formation of new 'episodic memories' (13,17,18), referred to as 'pattern separation' (19,20). Importantly, disruption of adult neurogenesis plays a key role in the pathogenesis of cognitive dysfunction. As such, a decrease in neurogenesis has been documented in neurodegenerative diseases, where mitochondrial dysfunction is a common attribute (8,21–23).

Mitochondrial dysfunction is a hallmark of many diseases that cause brain impairments and impinge on cognitive function, such as genetic mitochondrial disorders, neurodegenerative diseases and aging (24–27). Mitochondria are classically known to be the cells energy source, however, numerous studies have now uncovered divergent roles for mitochondria that go well beyond ATP production. In fact, our recent studies have unveiled the importance of mitochondria in neural stem cell commitment and fate decisions (4), suggesting that maintained mitochondrial function is not only essential in high-energy demanding post-mitotic neurons, but also during neurogenesis. The idea that mitochondria may be at the fundamental basis of brain function is clearly demonstrated by the progressive neurological dysfunction documented in human mitochondrial diseases (24,28,29). In fact, the organ most frequently affected in mitochondrial disorders, both in childhood and adult-onset forms, is the central nervous system, with clinical manifestations comprising of movement disorders, cognitive decline and even dementia (24,30,31). Furthermore, a recent study has demonstrated a strong correlation between age-dependent cognitive decline in monkeys and an increase prevalence of donut mitochondria that are hallmark of mitochondrial dysfunction (32,33). Despite the apparent importance of mitochondria within the brain (34–36), the exact role these organelles play during development and within the context of neurogenesis are not clear (37,38). Here we show that mitochondrial function is essential for brain development and the neurogenic process, both during embryonic development and in the adult brain. Using a genetic model of mitochondrial dysfunction, through deletion of the essential mitochondrial protein AIF in uncommitted neural progenitor cells, resulted in loss of NSC self-renewal, aberrant NPC proliferation, defects in cell cycle exit and neuronal differentiation. The resultant depletion of the adult NSC pool and defects in embryonic and adult neurogenesis lead to impairments of both motor and non-motor brain functions. In particular, disruption of mitochondrial function leads to severe defects in hippocampal-dependent cognitive function, such as memory and learning. These data present evidence that mitochondrial dysfunction is a major contributing factor in the cognitive decline observed in genetic neurological diseases.

Results

Establishing a model for mitochondrial dysfunction during forebrain development

The brain is the most affected organ in genetic disorders that impair mitochondrial function (24,39). Though mitochondrial dysfunction has a profound effect on motor and non-motor forebrain functions, the exact role mitochondria play in brain development in terms of neurogenesis is not clear. Thus, we were interested in elucidating the function of mitochondria during brain development and how the dysfunction of these organelles can manifest, over time, into cognitive impairments. For this reason, we first set out to unravel a possible developmental role for mitochondria during embryonic neurogenesis within the context of forebrain development. In order to study the effect of mitochondrial dysfunction on embryonic neurogenesis during forebrain/cortical development we aimed at creating an animal model that would recapitulate the mitochondrial defects observed in severe disease states, such as respiratory chain defects (including loss of complex 1), aberrant mitochondrial fragmentation and increased ROS production. Such a model was achieved by deletion of the mitochondrial oxidoreductase protein AIF, which has been previously shown to result in such attributes when deleted (40,41). AIF, an X-linked inner mitochondrial membrane protein and FAD-dependent NADH oxidase, was originally discovered as a component of caspase-independent cell death, and later revealed to be essential for normal mitochondrial function. Numerous studies have demonstrated that AIF deficiency results in impaired mitochondrial respiration and reduced expression of mitochondrial electron transport chain (ETC) complex I and complex III, as well as elevated ROS levels (41,42). The respiratory chain defects associated with AIF deficiency have been attributed to a resultant translational downregulation of complex I and III subunits due to loss of CHCHD4-dependent import (41,43–46). In addition and within the context of the brain, AIF loss in neurons results in severe mitochondrial fragmentation and disruption of cristae (40). AIF, not only plays an essential role in maintaining mitochondrial function and structure (40), but has been shown to cause neurodegeneration in mice when downregulated (47). More importantly, pathogenic mutations in AIF have been identified in humans with early-onset progressive severe mitochondrial encephalomyopathy with clinical manifestations of neurological and psychomotor developmental abnormalities (48,49).

The effect of mitochondrial dysfunction within the context of neurogenesis during cortical development was examined by generating an *in vivo* conditional genetic deletion of AIF in uncommitted cells of the early telencephalon (E9), prior to the onset of neurogenesis, using a Cre recombinase driven by the Foxg1 promoter. Loss of AIF (AIF-KO) was evident at the onset of embryonic neurogenesis (E12.5) (Fig. 1A and B), with a concomitant loss of Complex 1 (Fig. 1B), increased mitochondrial fragmentation in NPCs (Tbr2+ cells) (Fig. 1C and D) and increased production of ROS (reactive oxygen species) (Fig. 1E). The effect of AIF deletion on mitochondrial morphology was examined at mid-neurogenesis (E15.5) when the different populations of cells within the neurogenic lineage in the developing cortex are easily distinguished using specific markers. In this context, uncommitted and committed NPCs were identified by the markers Sox2 and Tbr2, respectively, and newborn neurons were identified by the marker Tuj1. By mid-neurogenesis, loss of AIF resulted in fragmentation of mitochondria in all cell populations of the developing cortex (Fig. 1F and G), including the uncommitted and committed populations of NPCs (Sox2+ and Tbr2+ cells) and the newborn neurons (DCX+ cells). In addition, there was a severe impairment in cristae architecture as observed by EM analysis showing a significant decrease in cristae number and diameter in cells obtained from the cortex of AIF knockout embryos when compared to the controls (Fig. 1H and I). Loss of AIF was also accompanied by decreased
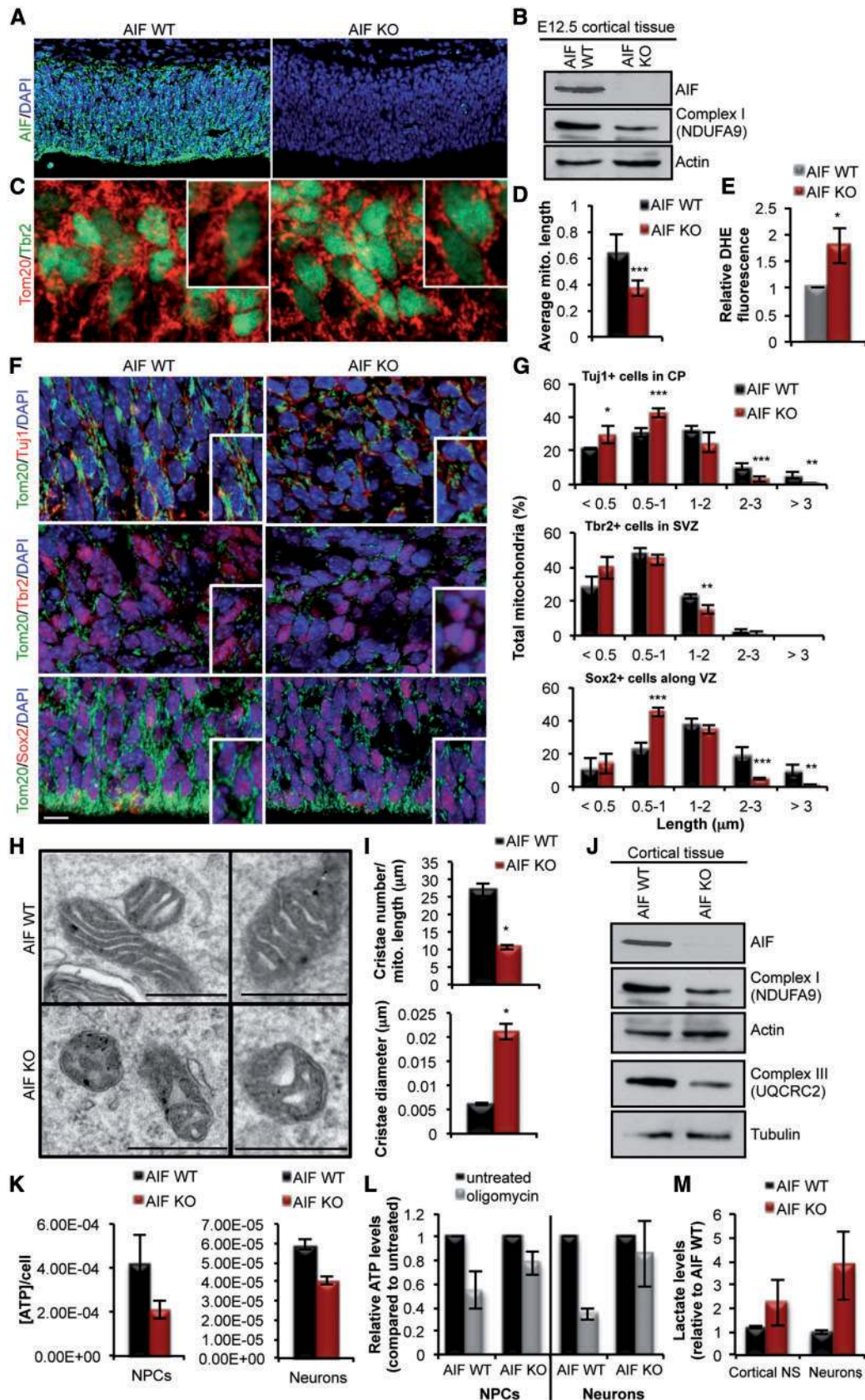
Figure 1. Conditional deletion of AIF causes loss of mitochondrial function in committed and uncommitted cells of the developing cortex. (**A** and **B**) Immunofluorescence and immunoblot analysis of AIF loss of expression in the cortex of E12.5 AIF-Foxg1Cre embryos compared to littermate controls. In (B) note the decreased expression of NDUFA9 (Complex 1) upon deletion of AIF. (**C**) Representative confocal images of mitochondrial morphology in coronal sections of AIF control or knockout brains at E12.5. Mitochondria and NPCs were visualized by Tom20 and Tbr2 immunostaining, respectively. (**D**) Average mitochondrial length measurements in AIF control and knockout cortices at E12.5. Represented as mean and SD ($n = 3$ independent samples). (**E**) Increased cytoplasmic ROS levels in AIF-KO E12.5

expression levels of components of Complex I and III of the ETC (Fig. 1J). Mitochondrial dysfunction was apparent in AIF-KO NPCs and neurons as indicated by decreased levels of total ATP, as well as, oligomycin-sensitive ATP levels (Fig. 1K and L). In addition, there was an increase in lactate levels in both NPCs and neurons indicating an increase reliance of AIF-KO cells on glycolysis (Fig. 1M). These data establish the loss of AIF as a model of mitochondrial dysfunction in both NPCs and neurons during embryonic cortical development.

Loss of mitochondrial function impairs cortical development

Next, we examined the consequence of mitochondrial dysfunction on cortical development as a whole. Firstly, AIF-KO embryos exhibited a visible thinning of the cortex and enlargement of the ventricle (Fig. 2A), demonstrating a defect in cortical development. Although there is a clear cortical defect in the AIF-KO cortex, DAPI staining revealed the formation of a clear cortical plate and Cux1 staining, which marks for layer 2/3 neurons, showed no detectable defect in neuronal migration or localization of layer 2/3 neurons (Fig. 2B). Since mitochondrial dysfunction is often associated with a global and general increase in cell death, cell survival in the cortex was first examined. Surprisingly, a significant increase in AC3+ apoptotic cells in the AIF-KO cortex was only observed within the cortical plate, a region populated by committed newborn neurons (Fig. 2C and D). The restriction of cell death in the AIF-KO cortex within the population of differentiating cells suggests that newborn neurons are highly sensitive to changes in mitochondrial function. These data highlight the importance of functional mitochondria in the generation of neurons and the lack of compensatory mechanisms during development, unlike what is observed following loss of AIF in mature post-mitotic neurons whereby survival is only affected following long-term loss of mitochondrial function (42). Furthermore, these data show that disruption of cortical development by mitochondrial dysfunction is not entirely due to a global increase in cell death, as there was apparent perturbation in the progenitor population, and cell survival was unaffected in the VZ (ventricular zone) and SVZ. Thus, we pursued a further investigation into a possible role for mitochondria during the neurogenic process.

Mitochondrial dysfunction causes defects in NPC self-renewal

In order to dissect the underlying cause of the cortical defect in AIF-KO animals several parameters were investigated that target the different processes occurring during neurogenesis, including NPC self-renewal, proliferation and differentiation. Given our previous study demonstrating a regulatory role for mitochondrial dynamics in neural stem cell fate decisions, we first examined the effect of mitochondrial dysfunction on the self-renewal capacity of NPCs. AIF-KO cortical cells showed a drastic inability to form neurospheres in culture (Fig. 2E) demonstrating that loss of AIF results in a severe impairment in the ability of neural stem cells to self-renew. Furthermore, *in vivo* measurement of the division angle of uncommitted Sox2+ anaphase cells along the VZ revealed that mitochondrial dysfunction, by loss of AIF, causes a significant increase in the number of cells undergoing asymmetric differentiative divisions, at the expense of symmetric self-renewing divisions (Fig. 2F). Together these data demonstrate that mitochondrial dysfunction impairs neural stem cell self-renewal.

Loss of mitochondrial function impairs NPC cell cycle exit and neuronal differentiation during embryonic neurogenesis

Though mitochondrial dysfunction promoted the commitment of NPCs, at the expense of self-renewal, the drastic decrease in cortical thickness suggested further underlying defects. Overall assessment of the proliferation capacity of cycling NPCs revealed an increased level of proliferation in AIF-KO cortices (Fig. 3A and B), as indicated by increased number of cells positive for the cell cycle markers PH3 (mitosis marker) and BrdU (S-phase marker). Further analysis of proliferation within the different population of cells during neurogenesis revealed an increased level of proliferation in the committed NPC population (Tbr2+ cells) (Fig. 3C and D). Interestingly, there was also ectopic proliferation in the DCX+ neuroblast population (Fig. 3C and D). This was particularly intriguing given that DCX+ cells represent a committed population of neuroblast cells that are exiting the cell cycle in order to complete the differentiation process. Given the severity of the defect at E15.5, the proliferation profile of neural progenitor and neuroblast cells was also examined at the onset of neurogenesis (E12.5) to determine the early affects of AIF loss. At this early stage, following only acute loss of AIF, a dysregulation in progenitor proliferation can be detected, as indicated by an increase in the percentage of Tbr2+/Ki67+ cells in AIF-KO brains compared to littermate controls (Fig. 3F). In addition, there is a significant increase in the number of newborn neurons that have sustained expression of the proliferative marker Ki67 (DCX+/Ki67+ cells) in AIF KO brains compared to their littermate controls (Fig. 3E and F). These observations suggested that proper mitochondrial function is required for regulation of cell proliferation and required for cell cycle exit and differentiation of neurons. Several approaches were utilized to confirm the hypothesis that mitochondrial dysfunction disrupts cell cycle exit and differentiation during neurogenesis. First, we used *in utero* electroporation of a GFP construct in order to track the fate of AIF-KO NPCs. This revealed that NPCs with dysfunctional mitochondria are more restricted to the intermediate zone of the cortex, with a decreased number of GFP+ cells within the cortical plate after 48hrs (Fig. 3G and H). In addition, there was a decreased number of GFP+ cells within the cortex of

cortical tissue relative to AIF littermate controls as measured by DHE fluorescence. (**F**) Representative confocal images of mitochondrial morphology in coronal sections of AIF control and knockout E15.5 developing cortex. Mitochondria were visualized by Tom20 and different cell populations during neurogenesis were visualized by immunostaining for Sox2 (uncommitted cells that contain NSCs), Tbr2 (committed progenitor cells) and Tuj1 (post-mitotic differentiated neurons). Insets represent zoomed views of mitochondria. Scale = 10 μm (VZ and SVZ; ventricular and subventricular zones, CP; cortical plate). (**G**) Mitochondrial length from (F) was quantified and binned into different length categories. Represented as mean and SD ($n = 3$ independent samples). (**H**) Representative EM images of mitochondrial ultrastructure from the indicated genotypes. Scale = 500 nm. (**I**) Cristae number and diameter from (H) were quantified and represented as mean and s.e.m. (**J**) Expression levels of components of Complex I and III of the ETC derived from AIF control and knockout cortical tissue at E15.5. (**K**) ATP measurements in NPCs and neurons cultured from AIF control and knockout cortical tissue at E15.5. Data represented as mean and s.e.m. ($n = 4$ for control; $n = 6$ for AIF KO). (**L**) ATP measurements relative to initial values (black) following 1-h oligomycin treatment (grey) in cultured NPCs and neurons from E15.5 cortical tissue. Mean and SD ($n = 4$ independent samples). (**M**) Lactate levels measured from similar conditions as (K). Mean and SD ($n = 3$ for control, $n = 5$ for AIF KO). $^*P < 0.05$; $^{**}P < 0.01$; $^{***}P < 0.001$ (Student's t-test).
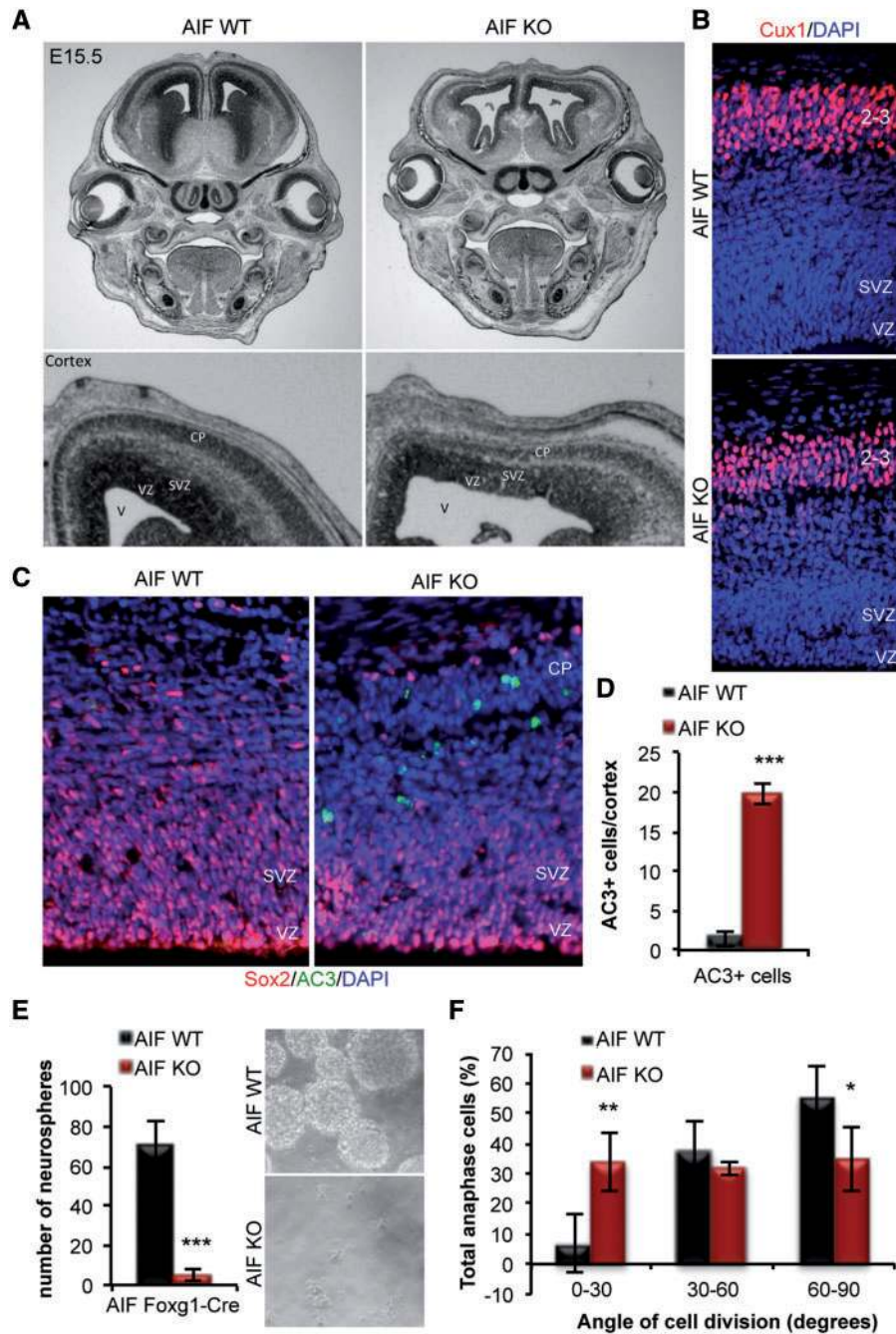
Figure 2. Impairment in mitochondrial function causes defects in neural stem cell self-renewal. (**A**) Representative images from coronal sections of E15.5 AIF control or knockout heads subjected to cresyl violet staining. (**B**) Representative images of E15.5 AIF control and knockout cortices stained with DAPI and Cux1, a marker of layer 2/3 neurons. (**C** and **D**) Representative confocal images of apoptotic cells (AC3 immunofluorescence) in E15.5 coronal sections from AIF control and knockout embryos. No co-localization of AC3 was observed in Sox2+ NPCs. Total number of AC3+ cells was counted in the entire cortex and graphed as mean and SD ($n = 3$ independent samples). (**E**) Primary neurosphere assay performed on cells derived from the dorsal cortex of E15.5 control and AIF knockout embryos. Data presented as mean and SD ($n = 5$ independent experiments). Representative phase images of neurospheres. (**F**) Measurements of the division angle of Sox2+ anaphase cells in coronal sections from E15.5 AIF control or knockouts. Mitotic spindle pole orientation of dividing uncommitted cells is associated with asymmetric versus symmetric divisions and cell fate determination. Horizontal (0–30°) and intermediate (30–60°) cleavage angles (yellow line), relative to the apical surface of the lateral vertical (LV, white line), correlate with asymmetric divisions, while vertical (60–90°) cleavage angles correlate with symmetric divisions. Chromatin was visualized by DAPI staining. Angles were measured, binned and presented as mean and SD ($n = 3$ individual samples). *$P < 0.05$; **$P < 0.01$; ***$P < 0.001$ (Student's t-test).

AIF-KO animal that were able to differentiate, as indicated by the decreased number of GFP+/DCX+ co-labelled cells (Fig. 3G and I). The effect of mitochondrial dysfunction on cell cycle exit and neuronal differentiation was further confirmed by an *in vitro* differentiation assay. Initiating differentiation of AIF-KO NPCs

in vitro showed a significant decrease in differentiated Tuj1+ neurons and maintained BrdU uptake in AIF-KO cells (Fig. 3J). Thus disruption of mitochondrial function causes a multifaceted defect and imposes a disruption at multiple stages of neurogenesis, from impaired self-renewal in the neural stem
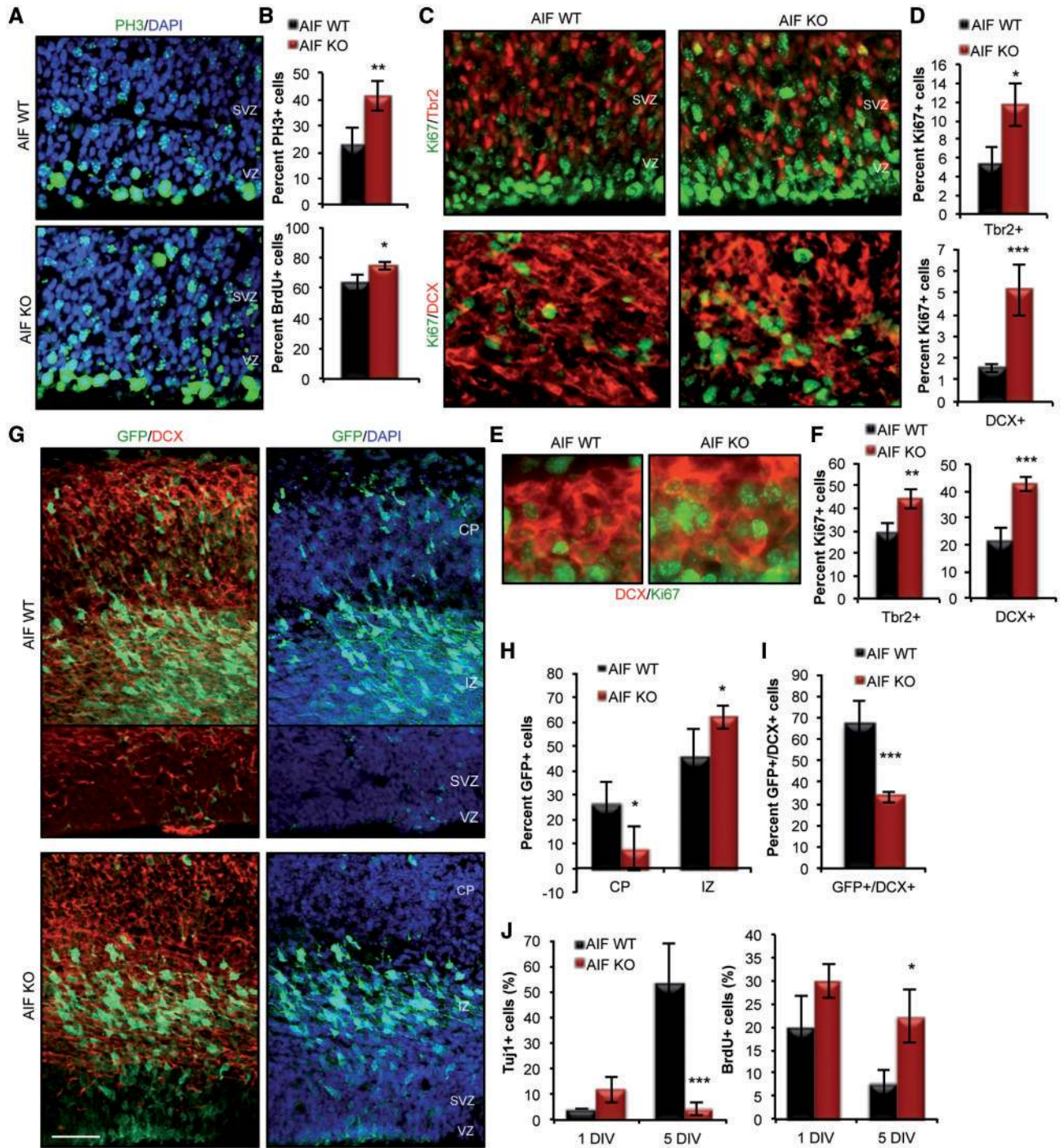
Figure 3. Mitochondrial dysfunction impairs multiple steps in the neurogenic process during cortical development. (**A** and **B**) Representative confocal images and quantification of proliferation of NPCs in E15.5 control and AIF knockouts using PH3 (phosphohistone 3; M-phase marker) and BrdU (S-phase marker) labeling. Data presented as mean and SD ($n = 3$ independent samples). (**C** and **D**) Representative confocal images and quantification of Tbr2+ progenitors and DCX+ neuroblasts co-labeled with Ki67 (proliferation marker) in E15.5 control and AIF knockouts. Data presented as mean and SD ($n = 3$ independent samples). (**E** and **F**) Representative confocal images and quantification of Tbr2+ progenitors and DCX+ neuroblasts co-labeled with Ki67 in E12.5 control and AIF knockouts. Data presented as mean and SD ($n = 3$ independent samples). (**G–I**) Representative confocal images following 48 h of *in utero* electroporation of GFP at E13.5 in the dorsal forebrain of control and AIF knockouts. Scale = 50 μm. Quantification of GFP+ cells based on location within the dorsal cortex (F) and co-labeling with DCX (G). Results are represented as mean and SD ($n = 3$ independent samples). (**J**) AIF control and knockout cells derived from E15.5 dorsal cortex were plated as monolayers and subjected to an *in vitro* differentiation assay. Cells were exposed to a 1-h BrdU pulse prior to fixation at 1 and 5 days *in vitro* (DIV). Data presented as mean and SD ($n = 3$ independent samples). *$P < 0.05$; **$P < 0.01$; ***$P < 0.001$ (Student's *t*-test).

cell population, followed by dysregulation of progenitor proliferation and a failure in the differentiation and survival of neurons.

Mitochondrial dysfunction impairs hippocampal development and leads to loss of NSCs and adult neurogenesis

Genetic diseases that result in mitochondrial abnormalities often show progressive clinical signs of impaired cognitive function. Generally, this impairment has been attributed to the degeneration of mature post-mitotic neurons. Based on our observations demonstrating a critical role for mitochondria in brain development and embryonic neurogenesis (Figs 2 and 3), we hypothesized that cognitive dysfunction may also arise due to defects in hippocampal development and formation of the dentate gyrus (DG), regions that are critical for learning and memory, as well as adult neurogenesis. In order to determine how mitochondrial dysfunction during development would manifest into adulthood, a conditional AIF knockout model that survives post-birth was generated where loss of AIF is restricted to the dorsal telencephalon using EMX1cre (Fig. 4A). Loss of AIF in NPCs within the dorsal embryonic telencephalon, using a conditional AIF-Emx1-Cre model exhibited mitochondrial dysfunction revealed by an increase in mitochondrial fragmentation in NPCs at E15.5 (Fig. 4B–D). This model showed a similar dysregulation in neural stem cell fate decisions with a decrease in symmetric self-renewing divisions (Fig. 4E), and increased progenitor proliferation (Fig. 4F). In addition, the AIF-Emx1Cre model recapitulated the defects in embryonic cortical development that was observed in the AIF-Foxg1Cre model, as observed by cortical thinning and enlarged ventricles at the end of neurogenesis (E18.5) and even into adulthood (10 weeks) (Fig. 4G). Analysis of the hippocampus revealed that although the onset of hippocampal development was evident at E18.5 in AIF-KO animals with the presence of uncommitted and committed NPCs (Sox2+ and Tbr2+ cells) (Fig. 4H), the progression and maturation of the hippocampus, including the DG, was impaired by 10 weeks of age when compared to the control animals (Fig. 4I). These data demonstrate that mitochondrial function is essential for hippocampal development and formation of the DG.

Neurogenesis is an ongoing process that continues in two regions of the adult brain, the SVZ (subventricular zone) of the lateral ventricle and the DG of the hippocampus. Recent studies have elegantly demonstrated that adult neural stem cells have an embryonic origin (50,51). Given the loss in stem cell self-renewal capacity, aberrant proliferation of NPCs and the defects observed in neuronal differentiation during embryonic development, we hypothesized that this would lead to depletion of the adult NPC pool and disruption of adult neurogenesis. Indeed, the embryonic defect in mitochondrial function manifested as a depletion of Sox2+ NPCs in the DG of the adult hippocampus (Fig. 4J and K). Furthermore, there was no indication of ongoing neurogenesis, as the AIF-KO DG had no detectable DCX+ newborn neurons at 10 weeks (Fig. 4J and K). These data highlight the fundamental role of mitochondria in the maturation of the hippocampus and for maintenance of adult neural stem cells and ongoing neurogenesis within the adult neurogenic zone.

Mitochondrial dysfunction causes cognitive deficits

Given that disruption in mitochondrial function is a common theme in aging and genetic diseases that affect cognition, we next asked whether sustained mitochondrial dysfunction would affect brain function. Behavioural evaluation of adult (10–11 weeks of age) AIF-KO animals began first with assessment of exploratory and locomoter activities. General locomotor activity, as assessed by the beam break test, showed no detectable difference in general motor activity of AIF-KO animals when compared to their littermate controls (Fig. 5A and B). Although, there was a trend towards increased activity in AIF-KO animals (Fig. 5B). Subjecting AIF-KO animals to an open field test, to assess their locomotor and exploratory behaviour, demonstrated that these animals had a tendency of avoiding the central areas of the open field and spent more time in the outer corners (Fig. 5C). Despite the increased time spent in the outer areas of the open field, no detectable deficit in sensorimotor activity was observed in the AIF-KO animals, in terms of velocity or distance travelled (Fig. 5C). Given the phenotypic defect observed in AIF-KO brains within the hippocampus and cortex, as well as the clinical presentation of motor and cognitive disruptions in mitochondrial diseases, AIF-KO animals were subjected to a series of behavioural tests intended in examining cortical and hippocampal functions. The rotarod test, which measures motor coordination, learning and balance, revealed a significant reduction in time on the rod for AIF-KO animals compared to their littermate controls, with limited ability to enhance their performance over the four trials each day (Fig. 5H). The results of the rotarod test suggest that AIF-KO adult animals exhibit motor dysfunction and a limited ability to learn the motor task. This is consistent with motor deficits observed in many neurodegenerative models and demonstrates that mitochondrial dysfunction is a major contributor to such a phenotype (45,52–56). Cognitive function in AIF-KO animals was assessed using the Morris water maze, which examines hippocampal-dependent spatial learning and memory. This test revealed a major deficit in hippocampal-dependent memory and learning in AIF-KO animals, demonstrating a complete inability of these animals to learn the location of the platform both during the training and with an associated lack of reference memory for the probe location during the probe test (Fig. 5D–F). This deficit was not due to a general locomotor (Fig. 5A–C) or visual deficit in AIF-KO. Cognitive function was assessed further using fear conditioning, which has been demonstrated to require the generation of new neurons through adult neurogenesis. Consistent with a defect in adult neurogenesis in AIF-KO animals, there was a significant impairment in contextual (hippocampal-dependent) memory, but not cued (amygdala-dependent) memory (Fig. 5G). These data demonstrate for the first time that mitochondrial dysfunction, as observed in many genetic and neurodegenerative diseases, is a major contributor to the clinical manifestation of cognitive impairment.

Discussion

Mitochondrial dysfunction is a common feature in many genetic diseases that affect brain function. Although it is clear that mitochondria are essential for cellular metabolism and neuronal survival, the exact role that mitochondria play in the etiology of these disorders and the ensuing motor and cognitive decline is not understood. Here we show that mitochondrial dysfunction emanating from the neural stem cell population propagates into a global impairment in forebrain development and neurogenesis in the embryonic and adult brain leading to a severe loss of motor and cognitive function. This study provides evidence that proper mitochondrial function is required in multiple cell populations, including neural stem, progenitor and
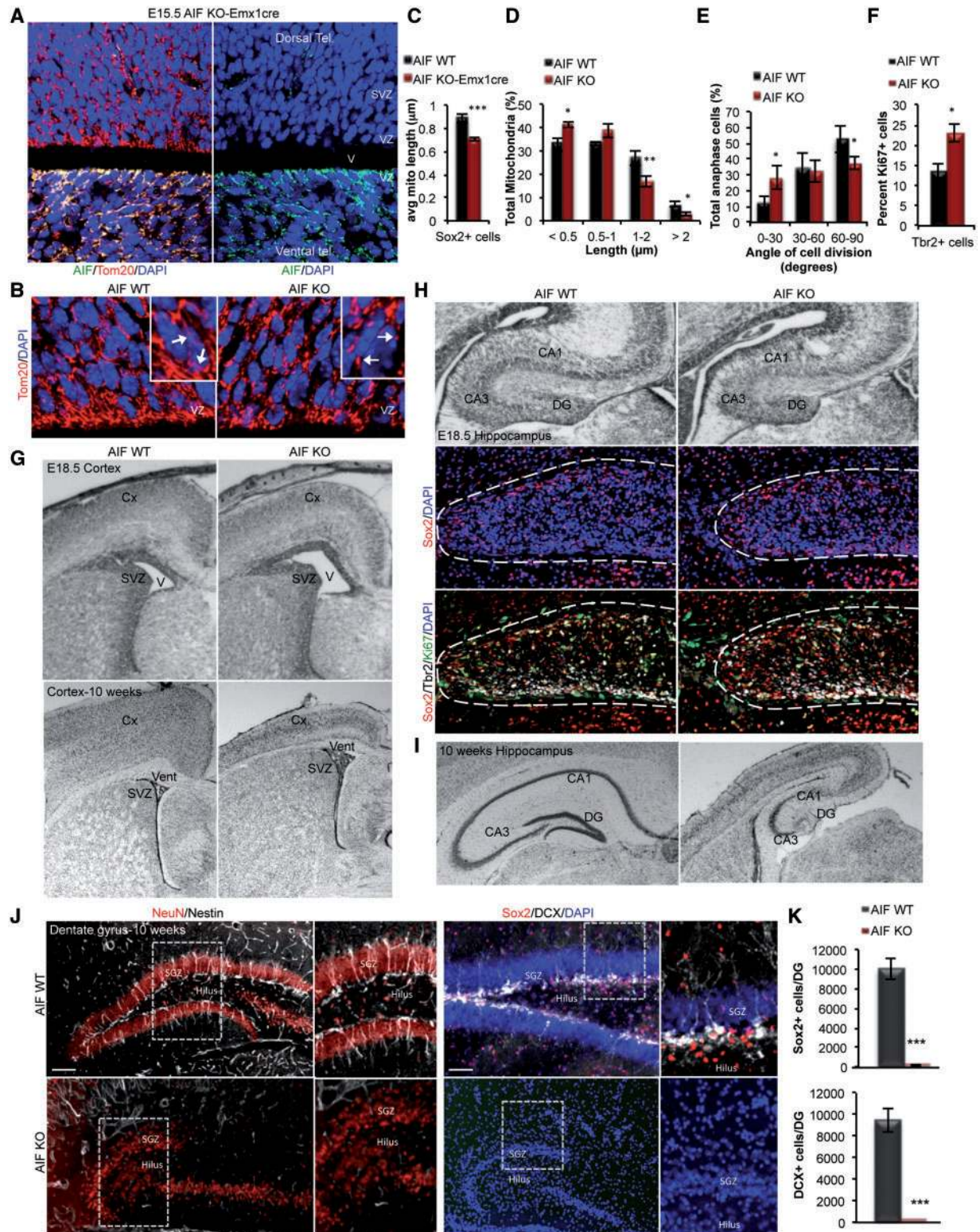
Figure 4. Loss of mitochondrial function causes age-dependent defects in forebrain development, depletion of NSCs and loss of adult neurogenesis in the DG. (**A**) Representative confocal images showing loss of AIF expression restricted to the dorsal cortex in AIF-Emx1Cre E15.5 embryos. (**B**) Representative confocal images of mitochondrial morphology in coronal sections of AIF control and knockout E15.5 developing cortex. Mitochondria were visualized by Tom20 and insets represent zoomed views of mitochondria. (VZ; ventricular zone). (**C** and **D**) Average mitochondrial length and mitochondrial length distribution from (B) was quantified and represented as mean and SD (*n* = 3 independent samples). (**E**) Measurements of the division angle of Sox2+ anaphase cells in E15.5 coronal sections for the indicated genotypes and presented as mean and SD (*n* = 3 independent samples). (**F**) Quantification of DCX+ neuroblasts co-labeled with Ki67 (proliferation marker) in E15.5 control and AIF knockouts. Data presented as mean and SD (*n* = 3 independent samples). (**G**) Cresyl violet stained coronal sections of E18.5 and 10-week adults with the indicated genotypes showing the cortex. (V; ventricle, SVZ; subventricular zones, Cx; cortex). (**H** and **I**) Cresyl violet stained coronal sections of E18.5 and 10-week adults showing the hippocampus. Representative confocal immunofluorescence images demonstrate zoomed views of the DG at E18.5 containing NPCs (Sox2 and Tbr2 labelled cells) (DG; dentate gyrus, vent; ventricle, svz; subventricular zones, Cx; cortex). (**J** and **K**) Representative confocal images of 10-week control and AIF knockout coronal sections of the dentate gyrus (DG) immunostained with Sox2 and Nestin (uncommitted cells), DCX (neuroblasts) and NeuN (mature neurons). Total Sox2+ and DCX+ cells in the entire DG was quantified and presented as mean and SD (*n* = 3 individual samples). Scale = 100 μm. *P < 0.05; ***P < 0.001 (Student's *t*-test).
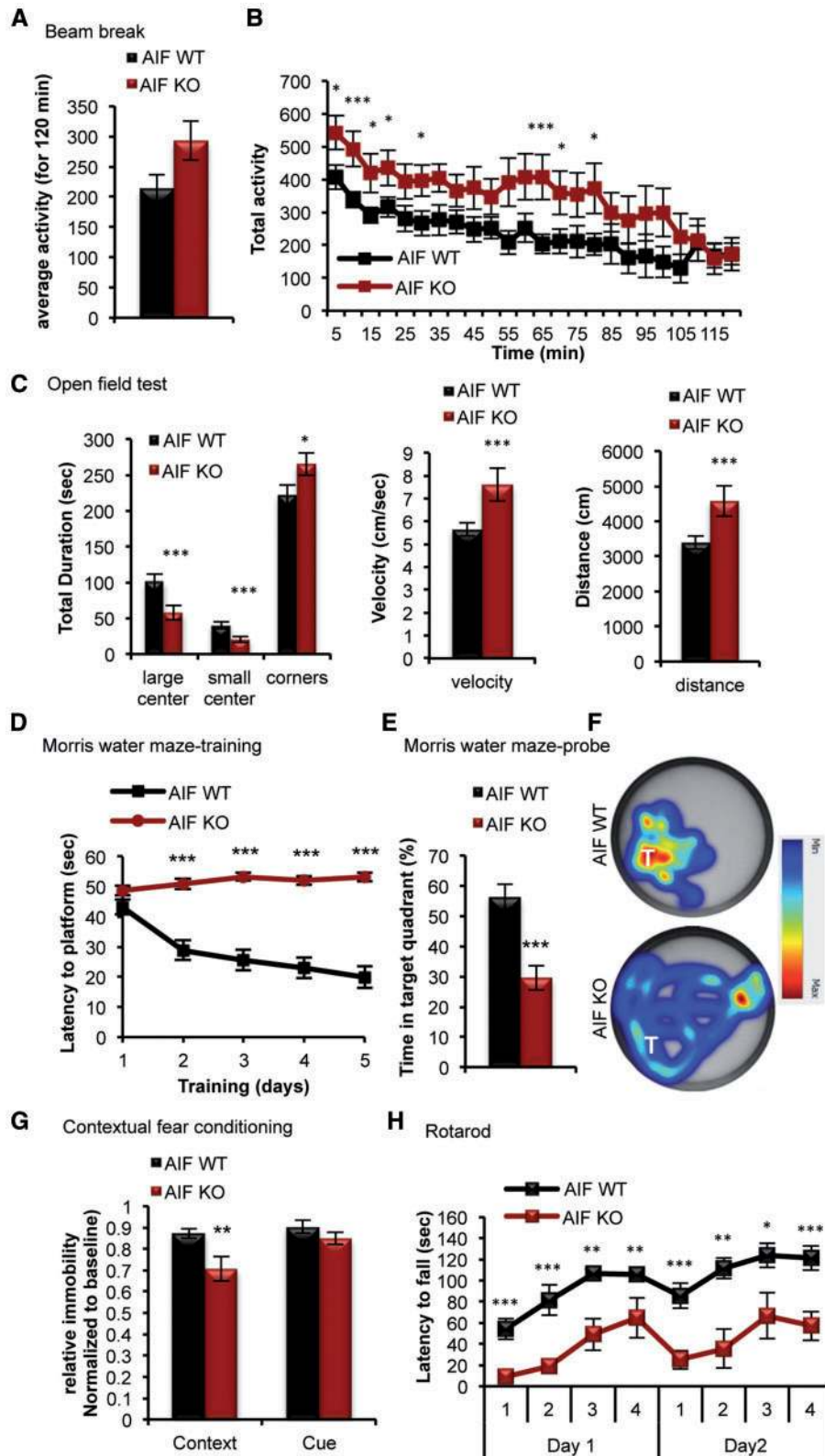
Figure 5. Mitochondrial dysfunction results in motor and cognitive deficits in adult mice. (**A** and **B**) Measurement of the overall activity of AIF-Emx1Cre knockouts and their littermate controls using the Beam break test at 10 weeks of age. Data presented as mean and s.e.m (using a 2-way repeated measures ANOVA Bonferroni post-hoc test). ($n = 20$ for control, $n = 14$ AIF KO). (**C**) Measurement of locomotor activity using the open field test. (**D–G**) Adult control and AIF knockout animals were subjected to hippocampal-dependent cognitive testing using the Morris water maze (D–F) and contextual fear conditioning (G). Data in (D) shows the Morris water maze training and data in (E) and (F) show the Morris water maze probe test at 11 weeks of age. For (D) data presented as mean and s.e.m (using a 2-way repeated measures ANOVA Bonferroni post-hoc test). For (E and G) data presented as mean and SD (using Student's t-test). (**H**) Graph showing the daily measurement of motor function by the rotorod test at 12 weeks of age in control and AIF-Emx1Cre knockout animals. Data presented as mean and s.e.m (using a 2-way repeated measures ANOVA Bonferroni post-hoc test). $^*P < 0.05$; $^{**}P < 0.01$; $^{***}P < 0.001$ (Student's t-test).
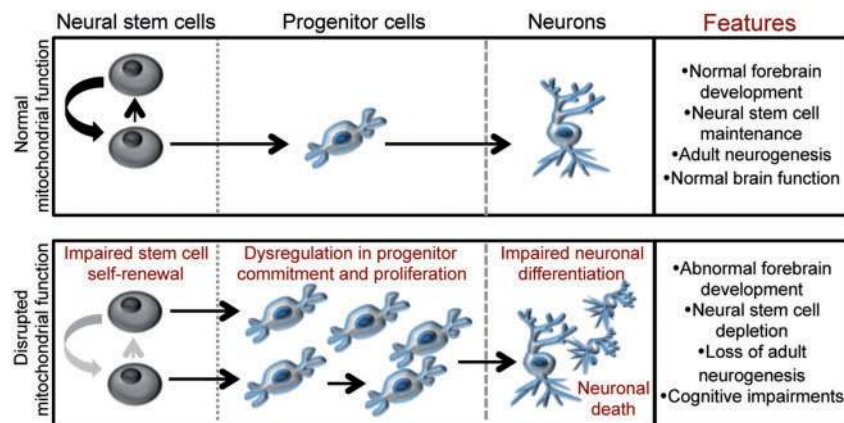
Figure 6. Mitochondrial function regulates the neurogenic process and is required for neural stem cell maintenance, neurogenesis and cognitive function. The cartoon depicts how the disruption of mitochondrial function within the uncommitted population of neural stem cells, as would occur in genetic mitochondrial-related disorders and neurodegenerative diseases, leads to defects in several steps of neurogenesis, including neural stem cell self-renewal and commitment, progenitor proliferation and neuronal differentiation. These defects culminate into abnormal brain development, depletion of the adult neural stem cell pool, loss of neurogenesis and cognitive defects.

neuroblast cells. Dysfunction of mitochondrial within these progressive cell populations during neurogenesis leads to an array of defects in stem cell self-renewal, progenitor proliferation and cell cycle exit and neuronal differentiation (Fig. 6). Together these defects culminate in abnormal forebrain development, with impaired cortical and hippocampal maturation, and a depletion of adult neural stem cells and loss of adult neurogenesis.

Mitochondrial diseases represent a group of multi-system genetic neurometabolic disorders with clinical manifestations most often detected in the CNS (24–27). Of the several clinical presentations observed in mitochondrial diseases, cognitive impairment is now increasingly recognized and diagnosed in human patients (27,29). However, little is known about the role mitochondria play in cognitive function. Interestingly, mitochondrial dysfunction has also been implicated in aging and in many neurodegenerative disorders, conditions that are strongly associated with cognitive decline (1–3). Though the decline in brain function in these conditions has been generally attributed to the side effect of neuronal cell death, our study now places mitochondrial dysfunction as the etiological factor leading to cognitive and motor impairments through its impact on stem cell maintenance and neurogenesis.

Neurogenesis is a complex and highly regulated process of neuronal generation that begins during embryonic brain development and continues into adulthood. The discovery of persistent neural stem cells and neurogenesis within the adult brain, a little over two decades ago, has revolutionized our understanding of brain homeostasis and function (10–13). Importantly, a decline in neurogenesis has been documented in conditions where cognitive decline is a major clinical component, including aging and neurodegenerative disorders, such Alzheimer's disease (57,58), however why this occurs is unknown. Though recent studies have suggested a role for mitochondria during neurogenesis how this may impact cognition has never been investigated. Using a genetic model of mitochondrial dysfunction within the forebrain, by deletion of the mitochondrial protein AIF, our study highlights the importance of mitochondria in the coordination of cell fate decisions during neurogenesis that go beyond a basic role in neuronal survival.

The process of neurogenesis consists of coordinated and highly regulated processes that eventually result in neuronal differentiation. Within this multi-step process several events must be coordinated, from commitment of neural stem cells to a neuronal lineage up to cell cycle exit and terminal differentiation of committed neuroblasts. Data here demonstrate that mitochondrial dysfunction causes a dysregulation of neural stem cell fate decisions, with a shift towards neuronal commitment at the expense of self-renewal. Given our previous findings, this defect is most likely due to increased ROS levels, which we have shown to activate a neuronal differentiation program. The loss of stem cell self-renewal capacity in AIF KO animals leads to an eventual depletion of the neural stem cell pool in the adult brain. Despite this apparent push towards neurogenesis, continued mitochondrial dysfunction within the committed progenitor population impairs the neurogenic process and leads to an overall decline in neurogenesis. This is due to the requisite need for proper mitochondrial function and metabolism in the regulation of cell cycle exit, differentiation and neuronal survival. Together, these defects prevent normal forebrain development in embryonic and post-natal brains, leading to severe cortical thinning, enlarged ventricles, and impaired hippocampal maturation and absence of a defined DG. Notably, loss of mitochondrial function during development results in severe brain dysfunction, with prominent motor and cognitive deficits.

The age-dependent accumulation of structural and functional defects observed in our study is reminiscent of the progressive nature of clinical manifestations observed in mitochondrial diseases (59). The model used in this study, through deletion of AIF, serves to represent the functional and phenotypic outcomes of severe cases of mitochondrial impairments. In the future, it would be interesting to model less severe mitochondrial impairments, which would be reminiscent of those found in human disease. However, it is not difficult to envision how less severe defects in mitochondrial function can result in similar impairments, albeit to a lesser extent. Furthermore, accumulation of mitochondrial dysfunction, over time, will result in compounded defects in the maintenance of a neural stem cell niche and ongoing neurogenesis within the adult brain. These results shed light

on the underlying cause of cognitive dysfunction in mitochondrial diseases, as well as aging and neurodegenerative disorders.

In conclusion, we have identified an essential role for mitochondria in the regulation of stem cell maintenance, neurogenesis and cognitive function. These results provide important insight into the outcome of mitochondrial dysfunction from a developmental perspective, as well as in the context of aging and neurodegenerative diseases.

Materials and Methods

Animals

Floxed AIF mice, originally obtained from Josef Penninger, and the telencephalon-specific *AIF-Foxg1Cre* conditional mutants have been previously described in Cheung *et al.* (2006) (40). To generate dorsal telencephalon-specific *AIF-Emx1Cre* conditional mutants floxed AIF homozygous female mice were bred with *Emx1-cre* mice. Littermate controls were used for all experiments. All experiments were approved by the University of Ottawa's Animal Care Ethics Committee adhering to the Guidelines of the Canadian Council on Animal Care.

Tissue processing and immunohistochemistry

For immunohistochemistry, sections were collected as 14 μm coronal cryosections or as 30 μm free-floating cryosections. In general, before antibody incubation, antigen retrieval was performed by heating sections at 95 °C for 30 min in DAKO retrieval solution, followed by 25 min at room temperature. When staining included Tom20 or Ki67, these incubation times were modified to 20 min DAKO followed by 10 min cooling, or 15 min DAKO and 5 min cooling, respectively. For BrdU incorporation, pregnant mice were given a single IP injection of 50 mg/kg BrdU and were harvested 2 h later. Sections were incubated in 2N HCl at 37 °C for 30 min and neutralized in 0.1M Na borate, pH8.5, for 15 min at room temperature. For immunofluorescence on cultured cells, cells seeded onto coverslips were fixed with 4% paraformaldehyde and stained as previously described (60). Primary antibodies used were Tom20 (Santa Cruz; sc-11415 and sc-17764), AIF (Abcam; ab32516), Sox2 (Santa Cruz, sc-17320), Tuj1 (Covance; PRB-435P), Tbr2 (eBioscience, 12-4875), DCX (Santa Cruz, sc-8066), NeuN (Millipore; MAB377), Ki67 (Cell Marque, SP6), PH3 (Millipore, 06-570), BrdU (Accurate Chemicals, OBT0030) and AC3 (Cell Signalling; 9664S).

Immunoblots

For total cell lysates, cells were washed with phosphate-buffered saline (PBS), lysed with 4% SDS in PBS, boiled for 5 min and the DNA was sheared by passage through a 26-gauge needle. Primary antibodies recognizing AIF (Abcam; ab32516), Complex I subunit NDUFA9 (Invitrogen; 459100), Complex III core protein 2 (UQCRC2, Abcam; ab14745) and Actin (Santa Cruz) were used. A secondary antibody conjugated to horseradish peroxidase (Jackson ImmunoResearch) was used and detected by Western Lightning Chemiluminescence Reagent Plus (Perkin Elmer).

ROS measurement

Embryonic E12.5 cortical tissue was manually dissociated in stem cell media. Single cells were washed and resuspended in Krebs Ringer Buffer (KRB, pH 7.4) containing 128 mM NaCl, 4.8 mM KCl, 1.2 mM MgSO$_4$, 1.2 mM KH$_2$PO$_4$, 10 mM glucose, 20 mM HEPES, 2.5 mM CaCl2 and 0.1% BSA. Cells were incubated in 1 μM DHE for 30 min at 37 °C (protected from light) followed by two washes with KRB. Cell suspensions were plated in 96-well black microplates and the fluorescence was then measured with a fluorescence plate reader at the excitation wavelength of 505 nm and an emission wavelength of 610 nm. Data were collected from multiple replicate wells for each experiment. Cell counts and viability under all conditions were determined by Trypan blue and PI staining, respectively. Florescence readings were normalized to cell number.

Mitochondrial length

Mitochondrial length was assessed by staining with Tom20 (translocase of outer mitochondria). Mitochondrial length was measured by tracing the mitochondria using ImageJ software. Mitochondrial length was either binned into different categories (<0.5 μm, 0.5–1 μm, 1–2 μm and >2 μm) or taken as an average.

Transmission electron microscopy (TEM) and cristae analysis

Mitochondrial ultrastructure was analyzed from whole cells of cultured cortical neurons isolated from wild-type and AIF knockout cortices at E15.5. Briefly, plated neurons were rapidly washed in PBS and harvested by scraping very lightly. Neurons were fixed in 2% gluteraldehyde for 20 min at room temperature and stored immediately at 4 °C for processing as previously described (40). Cristae analysis was performed using ImageJ and a minimum of 100 mitochondria were analyzed. For each individual cristae, the average diameter was measured from three representative regions.

In vitro cultures

Cells were obtained by dissection of the dorsal (cortex) telencephalic tissue of developing embryos. Neurospheres and cortical neuronal cultures were performed as previously described (60,61). Cortical neurons were seeded on plates coated with 0.01 mg/ml poly-D-lysine (BD Bioscience) and maintained in Neurobasal media (Gibco) that contained 2% B27 (Gibco), 1% N2 (Gibco), 0.6 mM L-glutamine (Gibco) and 1% Pen-Strep (Sigma). For neurosphere cultures, cells were plated at a density of 40 cells/μl and maintained for a maximum of 6 days in Stem cell Media (SCM) containing DMEM/F12 (Sigma) supplemented with 2% B27, 1% Pen-Strep, 12.5 ng/ml EGF, 12.5 ng/ml bFGF (Sigma) and 2 ng/μl heparin (sigma). Cultures were replenished with fresh media (doubling the volume) at day 3. Primary neurosphere assays were plated at a clonal density of 10 cells/μl in 24-well plates (six wells were plated per condition) and neurospheres were counted at day 5–7. *In vitro* differentiation assays were performed by plating cells at a density of 1.0×10^5 cells/well of a 24-well plate with coverslips coated with laminin and poly-L-ornithine in Monolayer media containing DMEM/F12 media supplemented with 1% N2, 1% Pen-Strep, 12.5 ng/ml EGF, 2.5 ng/ml bFGF and 2 ng/μl heparin. After 2 days, differentiation was initiated by changing the media to DMEM/F12 supplemented with 1% FBS, 1% N2, 1% Pen-Strep and 2 ng/μl heparin. At different days post-differentiation and prior to fixation for analysis, cells were subjected to a 1-h BrdU pulse.

ATP assay

ATP concentrations were measured with the CellTiter-Glo Luminescent Assay (Promega) using a LUMIstar Galaxy

luminometer (BMG Labtechnologies) according to manufacturer's protocol. Data were collected from multiple replicate wells for each experiment. Viability of cells under all conditions was ensured by PI staining.

Lactate measurements

Lactate release was measured by analysis of media using the Lactate Standard Set (Trinity Biotech) according to manufacturer's protocol. Lactate concentration from neurosphere and neuronal cultures were compared between start and final media (i.e. day of seeding and last day of culture). All assays were performed in triplicates and normalized to cell number. Viability of cells under all conditions was ensured by PI staining.

Anaphase cell division angle

Mitotic spindle pole orientation of uncommitted cells is associated with asymmetric versus symmetric divisions and cell fate determination. The plane of division of Sox2 anaphase cells was quantified as previously described (62). Briefly, E12.5 or E15.5 cortical sections were stained with Sox2 and DAPI to visualize chromatin. Sox2 cells undergoing anaphase were imaged along the apical surface of the lateral ventricle. Using ImageJ to quantify the angle of division, one line was drawn to trace the surface of ventricle and a second line traced the cleavage furrow. The smallest angle formed between the two intersecting lines was calculated. Angle measurements were binned into three categories of cleavage planes: Vertical cleavage planes (60–90°), horizontal (0–30°) and intermediate (30–60°). Horizontal (0–30°) and intermediate (30–60°) cleavage angles, relative to the apical surface of the lateral vertical correlate with asymmetric divisions and vertical (60–90°) cleavage angles correlate with symmetric divisions.

Cell counts

For embryonic counts, cells expressing the marker of interest were quantified along the entire length of the dorsal cortex. Regions of the VZ, SVZ and CP were delineated by Sox2, Tbr2 and DCX staining, respectively. Counts specified for Sox2+ uncommitted cells were restricted to a region 20–30 μm away from the lateral ventricle and spanning the entire length of the cortex. For adult counts within the DG, Sox2+ and DCX+ cells in the SGZ were quantified in every 9th section (40 μm) throughout the rostral-caudal length of the DG, and the sum of positive cells from all sections was multiplied by 9 to obtain the estimated total cell number per DG. All counts were performed using imageJ.

In utero electroporation

In utero electroporations were performed as previously described in Khacho *et al.* (4). Briefly, pups of pregnant *AIF-floxed* females crossed with male *Foxg1Cre* males were electroporated at E13.5 with plasmids containing GFP. The GFP plasmid was prepared using the Qiagen Megaprep Kit, diluted to 2 μg/μl in sterile H2O and mixed with trace amounts of Trypan Blue dye. The plasmid was injected into the lateral ventricle of the embryonic brain using an Eppendorf Femtojet Microinjector and electroporated into the dorsolateral cortex using a BTX ECM 830 Square Wave Electroporator. Animals were sacrificed 2 days later at E15.5. For analysis, 14 μm coronal sections from electroporated brains were selected based on equivalent rostro-caudal levels of the brain, relative to the corpus callosum and anterior commisure. Visualization of GFP was achieved by treating tissue sections with hot, non-boiling citric acid for 15 min and staining with antibodies against GFP. Amplification was performed on the GFP signal using the Avidin-Biotin Complex (ABC) kit according to the manufacturer's protocol (Vector Laboratories).

Behavioural tests

Activity monitoring
Locomotor activity over a 2-h period was measured in a novel home cage and recorded as number of infrared beam as analyzed by the MicroMax system (Accuscan).

Open field test
The mice were placed in a corner of the square arena (45-cm long on each side and 45-cm high) and allowed to explore the new environment for a total of 10 min at light levels of 300 lux. Mouse movements were videotaped and the time spent in the center (24 × 15 cm) and corners (squares with 10-cm sides) of the OF arena was analyzed using by Ethovision 10 XT video tracking system (Noldus Information Technology, North America).

Fear conditioning analysis
Fear conditioning experiments were performed using the PhenoTyper box and Ethovision 10 XT video tracking system (Noldus Information Technology, North America) as previously described (63) with minor modifications. The method used for the fear conditioning test including the use of the foot shock sensitivity test to determine optimal shock (62). Briefly, on day 1 for training mice receiving after 2 min, a 30 s, 90 dB tone co-terminating in a 2 s, 0.45 mA foot-shock. This was repeated a second time after a 1 min inter-stimulus interval and then the mice were removed from the box after a total of 6 min. Approximately 24 h after training, the contextually conditioned fear testing was performed by placing the mice back into the same apparatus for a total duration of 6 min. Approximately 48 h after training, cue conditioned fear testing was performed into a new context were they were allowed to freely explore the box for 3 min before re-exposure to the fear conditioning tone for a duration of 3 min. For the cue test the context of testing was modified by changing the interior shape of the apparatus, floor and wall texture of the apparatus, not playing white noise in the testing room, adding a vanilla odor and using a different handling technique to place mice into the box.

Morris water maze
The water maze was performed using the mouse water maze and Ethovision 10 XT video tracking system (Noldus Information Technology, North America). The protocol was previously described Qin *et al.* (64) with the exception that the mice were trained for 5 days instead of 9 days. Briefly the pool was filled with opaque water, the water was heated at 21 °C, and a white platform was submerged 1 cm below the water's surface in the center of the target quadrant. Mice were randomly placed on one of four starting points in one of the four quadrants and given 60 s to find the hidden platform. Mice that did not find the platform at the end of the 60 s period were led to the platform and were allowed to stay there for 20 s. Each mouse performed four trials per day with an inter-trial interval of 20 mins for

5 consecutive days. On the 6th day, the platform was removed from the pool and mice were given one 60 s trial at one of four random start locations.

Rotorod

Motor function was assessed using an accelerating rotorod (IITC Life Science, USA) that was set to accelerate from 0 to 45 rpm in 300 s. Mice were evaluated for 4 trials per session on two consecutive days, with a 30 min trial interval. The trial was ended when mice fell off the rod and for each trial the latency to fall was recorded.

For all behavioral tests, male mice for the wild-type and AIF knockout genotype were used. In addition, there were no apparent growth abnormalities of AIF KO mice when compared to their littermate controls.

Statistical analysis

Statistical comparisons in this study were performed using an unpaired two-tailed *t*-test. For behavioural tests, statistical analysis was performed using ANOVA. Differences were considered significant with a P-value of <0.05 (*), $**P < 0.01$, $***P < 0.001$.

Author Contributions

All authors reviewed the manuscript. M.K. designed and performed experiments, analyzed data and wrote the paper; A.C. assisted and performed experiments, and maintained mice colonies; D.S. assisted with *in vivo* experiments; J.G.M. provided technical assistance; D.C.L. supervised behavioural experiments and interpreted the behavioural data; D.S.P. provided reagents and interpreted the data; and R.S.S. designed experiments, interpreted the data, supported and directed the research.

Acknowledgements

Conflict of Interest statement. None declared.

References

1. Khacho, M. and Slack, R.S. (2015) Mitochondrial dynamics in neurodegeneration: from cell death to energetic states. *AIMS Mol. Sci.*, **2**, 161–174.
2. Nunnari, J. and Suomalainen, A. (2012) Mitochondria: in sickness and in health. *Cell*, **148**, 1145–1159.
3. Lin, M.T. and Beal, M.F. (2006) Mitochondrial dysfunction and oxidative stress in neurodegenerative diseases. *Nature*, **443**, 787–795.
4. Khacho, M., Clark, A., Svoboda, D.S., Azzi, J., MacLaurin, J.G., Meghaizel, C., Sesaki, H., Lagace, D.C., Germain, M., Harper, M.E. *et al*. (2016) Mitochondrial dynamics impacts stem cell identity and fate decisions by regulating a nuclear transcriptional program. *Cell Stem Cell*, **19**, 232–247.
5. Hu, C., Fan, L., Cen, P., Chen, E., Jiang, Z. and Li, L. (2016) Energy metabolism plays a critical role in stem cell maintenance and differentiation. *Int. J. Mol. Sci.*, **17**, 253.
6. Folmes, C.D., Dzeja, P.P., Nelson, T.J. and Terzic, A. (2012) Metabolic plasticity in stem cell homeostasis and differentiation. *Cell Stem Cell*, **11**, 596–606.
7. Zhang, J., Nuebel, E., Daley, G.Q., Koehler, C.M. and Teitell, M.A. (2012) Metabolic regulation in pluripotent stem cells during reprogramming and self-renewal. *Cell Stem Cell*, **11**, 589–595.
8. Baker, S.A., Baker, K.A. and Hagg, T. (2004) Dopaminergic nigrostriatal projections regulate neural precursor proliferation in the adult mouse subventricular zone. *Eur. J. Neurosci.*, **20**, 575–579.
9. Raber, J., Rola, R., LeFevour, A., Morhardt, D., Curley, J., Mizumatsu, S., VandenBerg, S.R. and Fike, J.R. (2004) Radiation-induced cognitive impairments are associated with changes in indicators of hippocampal neurogenesis. *Radiat. Res.*, **162**, 39–47.
10. Duan, X., Kang, E., Liu, C.Y., Ming, G.L. and Song, H. (2008) Development of neural stem cell in the adult brain. *Curr. Opin. Neurobiol.*, **18**, 108–115.
11. Gage, F.H. (2000) Mammalian neural stem cells. *Science*, **287**, 1433–1438.
12. Cameron, H.A. and McKay, R.D. (2001) Adult neurogenesis produces a large pool of new granule cells in the dentate gyrus. *J. Comp. Neurol.*, **435**, 406–417.
13. Aimone, J.B., Deng, W. and Gage, F.H. (2010) Adult neurogenesis: integrating theories and separating functions. *Trends Cogn. Sci.*, **14**, 325–337.
14. Lacar, B., Parylak, S.L., Vadodaria, K.C., Sarkar, A. and Gage, F.H. (2014) Increasing the resolution of the adult neurogenesis picture. *F1000Prime Rep.*, **6**, 8.
15. Ernst, A., Alkass, K., Bernard, S., Salehpour, M., Perl, S., Tisdale, J., Possnert, G., Druid, H. and Frisen, J. (2014) Neurogenesis in the striatum of the adult human brain. *Cell*, **156**, 1072–1083.
16. Kitamura, T., Saitoh, Y., Takashima, N., Murayama, A., Niibori, Y., Ageta, H., Sekiguchi, M., Sugiyama, H. and Inokuchi, K. (2009) Adult neurogenesis modulates the hippocampus-dependent period of associative fear memory. *Cell*, **139**, 814–827.
17. Stone, S.S., Teixeira, C.M., Devito, L.M., Zaslavsky, K., Josselyn, S.A., Lozano, A.M. and Frankland, P.W. (2011) Stimulation of entorhinal cortex promotes adult neurogenesis and facilitates spatial memory. *J. Neurosci.*, **31**, 13469–13484.
18. Deng, W., Aimone, J.B. and Gage, F.H. (2010) New neurons and new memories: how does adult hippocampal neurogenesis affect learning and memory?. *Nat. Rev. Neurosci.*, **11**, 339–350.
19. Sahay, A., Scobie, K.N., Hill, A.S., O'Carroll, C.M., Kheirbek, M.A., Burghardt, N.S., Fenton, A.A., Dranovsky, A. and Hen, R. (2011) Increasing adult hippocampal neurogenesis is sufficient to improve pattern separation. *Nature*, **472**, 466–470.
20. Danielson, N.B., Kaifosh, P., Zaremba, J.D., Lovett-Barron, M., Tsai, J., Denny, C.A., Balough, E.M., Goldberg, A.R., Drew, L.J., Hen, R. *et al.* (2016) Distinct contribution of adult-born hippocampal granule cells to context encoding. *Neuron*, **90**, 101–112.
21. Li, B., Yamamori, H., Tatebayashi, Y., Shafit-Zagardo, B., Tanimukai, H., Chen, S., Iqbal, K. and Grundke-Iqbal, I. (2008)

Failure of neuronal maturation in Alzheimer disease dentate gyrus. *J. Neuropathol. Exp. Neurol.*, **67**, 78–84.

22. Zhao, C., Deng, W. and Gage, F.H. (2008) Mechanisms and functional implications of adult neurogenesis. *Cell*, **132**, 645–660.

23. O'Keeffe, G.C., Tyers, P., Aarsland, D., Dalley, J.W., Barker, R.A. and Caldwell, M.A. (2009) Dopamine-induced proliferation of adult neural precursor cells in the mammalian subventricular zone is mediated through EGF. *Proc. Natl. Acad. Sci. U S A.*, **106**, 8754–8759.

24. Finsterer, J. (2012) Cognitive dysfunction in mitochondrial disorders. *Acta Neurol. Scand.*, **126**, 1–11.

25. Beal, M.F. (2005) Mitochondria take center stage in aging and neurodegeneration. *Ann. Neurol.*, **58**, 495–505.

26. Kwong, J.Q., Beal, M.F. and Manfredi, G. (2006) The role of mitochondria in inherited neurodegenerative diseases. *J. Neurochem.*, **97**, 1659–1675.

27. Valenti, D., de Bari, L., De Filippis, B., Henrion-Caude, A. and Vacca, R.A. (2014) Mitochondrial dysfunction as a central actor in intellectual disability-related diseases: an overview of Down syndrome, autism, Fragile X and Rett syndrome. *Neurosci. Biobehav. Rev.*, **46 Pt 2**, 202–217.

28. Rajnish, K. and Chaturvedi, M.F.B. (2013) Mitochondrial diseases of the brain. *Free Radic. Biol. Med.*, **63**, 1–29.

29. Falk, M.J. (2010) Neurodevelopmental manifestations of mitochondrial disease. *J. Dev. Behav. Pediatr.*, **31**, 610–621.

30. Zeviani, M. and Di Donato, S. (2004) Mitochondrial disorders. *Brain*, **127**, 2153–2172.

31. Andre Mattman, S.S., Mezei, M.M., Salvarinova-Zivkovic, R., Alfadhel, M. and Lillquist, Y. (2011) Mitochondrial disease clinical manifestations: an overview. *BC Med. J.*, **53**, 183–187.

32. Hara, Y., Yuk, F., Puri, R., Janssen, W.G., Rapp, P.R. and Morrison, J.H. (2014) Presynaptic mitochondrial morphology in monkey prefrontal cortex correlates with working memory and is improved with estrogen treatment. *Proc. Natl. Acad. Sci. U S A.*, **111**, 486–491.

33. Picard, M. and McEwen, B.S. (2014) Mitochondria impact brain function and cognition. *Proc. Natl. Acad. Sci. U S A.*, **111**, 7–8.

34. Calingasan, N.Y., Ho, D.J., Wille, E.J., Campagna, M.V., Ruan, J., Dumont, M., Yang, L., Shi, Q., Gibson, G.E. and Beal, M.F. (2008) Influence of mitochondrial enzyme deficiency on adult neurogenesis in mouse models of neurodegenerative diseases. *Neuroscience*, **153**, 986–996.

35. Voloboueva, L.A. and Giffard, R.G. (2011) Inflammation, mitochondria, and the inhibition of adult neurogenesis. *J. Neurosci. Res.*, **89**, 1989–1996.

36. Xavier, J.M., Rodrigues, C.M. and Sola, S. (2016) Mitochondria: major regulators of neural development. *Neuroscientist*, **22**, 346–358.

37. Ishimura, R., Martin, G.R. and Ackerman, S.L. (2008) Loss of apoptosis-inducing factor results in cell-type-specific neurogenesis defects. *J. Neurosci.*, **28**, 4938–4948.

38. Wang, W., Esbensen, Y., Kunke, D., Suganthan, R., Rachek, L., Bjoras, M. and Eide, L. (2011) Mitochondrial DNA damage level determines neural stem cell differentiation fate. *J. Neurosci.*, **31**, 9746–9751.

39. Finsterer, J. (2006) Central nervous system manifestations of mitochondrial disorders. *Acta Neurol. Scand.*, **114**, 217–238.

40. Cheung, E.C., Joza, N., Steenaart, N.A., McClellan, K.A., Neuspiel, M., McNamara, S., MacLaurin, J.G., Rippstein, P., Park, D.S., Shore, G.C. et al. (2006) Dissociating the dual roles of apoptosis-inducing factor in maintaining mitochondrial structure and apoptosis. *EMBO J.*, **25**, 4061–4073.

41. Vahsen, N., Cande, C., Briere, J.J., Benit, P., Joza, N., Larochette, N., Mastroberardino, P.G., Pequignot, M.O., Casares, N., Lazar, V. et al. (2004) AIF deficiency compromises oxidative phosphorylation. *EMBO J.*, **23**, 4679–4689.

42. Germain, M., Nguyen, A.P., Khacho, M., Patten, D.A., Screaton, R.A., Park, D.S. and Slack, R.S. (2013) LKB1-regulated adaptive mechanisms are essential for neuronal survival following mitochondrial dysfunction. *Hum. Mol. Genet.*, **22**, 952–962.

43. Hangen, E., Feraud, O., Lachkar, S., Mou, H., Doti, N., Fimia, G.M., Lam, N.V., Zhu, C., Godin, I., Muller, K. et al. (2015) Interaction between AIF and CHCHD4 regulates respiratory chain biogenesis. *Mol. Cell*, **58**, 1001–1014.

44. Brown, D., Yu, B.D., Joza, N., Benit, P., Meneses, J., Firpo, M., Rustin, P., Penninger, J.M. and Martin, G.R. (2006) Loss of Aif function causes cell death in the mouse embryo, but the temporal progression of patterning is normal. *Proc. Natl. Acad. Sci. U S A.*, **103**, 9918–9923.

45. Benit, P., Goncalves, S., Dassa, E.P., Briere, J.J. and Rustin, P. (2008) The variability of the harlequin mouse phenotype resembles that of human mitochondrial-complex I-deficiency syndromes. *PLoS One*, **3**, e3208.

46. Pospisilik, J.A., Knauf, C., Joza, N., Benit, P., Orthofer, M., Cani, P.D., Ebersberger, I., Nakashima, T., Sarao, R., Neely, G. et al. (2007) Targeted deletion of AIF decreases mitochondrial oxidative phosphorylation and protects from obesity and diabetes. *Cell*, **131**, 476–491.

47. Klein, J.A., Longo-Guess, C.M., Rossmann, M.P., Seburn, K.L., Hurd, R.E., Frankel, W.N., Bronson, R.T. and Ackerman, S.L. (2002) The harlequin mouse mutation downregulates apoptosis-inducing factor. *Nature*, **419**, 367–374.

48. Ghezzi, D., Sevrioukova, I., Invernizzi, F., Lamperti, C., Mora, M., D'Adamo, P., Novara, F., Zuffardi, O., Uziel, G. and Zeviani, M. (2010) Severe X-linked mitochondrial encephalomyopathy associated with a mutation in apoptosis-inducing factor. *Am. J. Hum. Genet.*, **86**, 639–649.

49. Rinaldi, C., Grunseich, C., Sevrioukova, I.F., Schindler, A., Horkayne-Szakaly, I., Lamperti, C., Landoure, G., Kennerson, M.L., Burnett, B.G., Bonnemann, C. et al. (2012) Cowchock syndrome is associated with a mutation in apoptosis-inducing factor. *Am. J. Hum. Genet.*, **91**, 1095–1102.

50. Furutachi, S., Miya, H., Watanabe, T., Kawai, H., Yamasaki, N., Harada, Y., Imayoshi, I., Nelson, M., Nakayama, K.I., Hirabayashi, Y. et al. (2015) Slowly dividing neural progenitors are an embryonic origin of adult neural stem cells. *Nat. Neurosci.*, **18**, 657–665.

51. Fuentealba, L.C., Rompani, S.B., Parraguez, J.I., Obernier, K., Romero, R., Cepko, C.L. and Alvarez-Buylla, A. (2015) embryonic origin of postnatal neural stem cells. *Cell*, **161**, 1644–1655.

52. Nuber, S., Petrasch-Parwez, E., Winner, B., Winkler, J., von Horsten, S., Schmidt, T., Boy, J., Kuhn, M., Nguyen, H.P., Teismann, P. et al. (2008) Neurodegeneration and motor dysfunction in a conditional model of Parkinson's disease. *J. Neurosci.*, **28**, 2471–2484.

53. Rousseaux, M.W., Marcogliese, P.C., Qu, D., Hewitt, S.J., Seang, S., Kim, R.H., Slack, R.S., Schlossmacher, M.G., Lagace, D.C., Mak, T.W. et al. (2012) Progressive dopaminergic cell loss with unilateral-to-bilateral progression in a genetic model of Parkinson disease. *Proc. Natl. Acad. Sci. U S A.*, **109**, 15918–15923.

54. Knippenberg, S., Thau, N., Dengler, R. and Petri, S. (2010) Significance of behavioural tests in a transgenic mouse

model of amyotrophic lateral sclerosis (ALS). *Behav. Brain Res.*, **213**, 82–87.

55. Carter, R.J., Lione, L.A., Humby, T., Mangiarini, L., Mahal, A., Bates, G.P., Dunnett, S.B. and Morton, A.J. (1999) Characterization of progressive motor deficits in mice transgenic for the human Huntington's disease mutation. *J. Neurosci.*, **19**, 3248–3257.

56. Breuer, M.E., Willems, P.H., Russel, F.G., Koopman, W.J. and Smeitink, J.A. (2012) Modeling mitochondrial dysfunctions in the brain: from mice to men. *J. Inherit. Metab. Dis.*, **35**, 193–210.

57. Martinez-Canabal, A. (2014) Reconsidering hippocampal neurogenesis in Alzheimer's disease. *Front Neurosci.*, **8**, 147.

58. Seib, D.R. and Martin-Villalba, A. (2015) Neurogenesis in the normal ageing hippocampus: a mini-review. *Gerontology*, **61**, 327–335.

59. Goldstein, A.C., Bhatia, P. and Vento, J.M. (2013) Mitochondrial disease in childhood: nuclear encoded. *Neurotherapeutics*, **10**, 212–226.

60. Khacho, M., Tarabay, M., Patten, D., Khacho, P., MacLaurin, J.G., Guadagno, J., Bergeron, R., Cregan, S.P., Harper, M.E., Park, D.S. *et al.* (2014) Acidosis overrides oxygen deprivation to maintain mitochondrial function and cell survival. *Nat. Commun.*, **5**, 3550.

61. Vanderluit, J.L., Ferguson, K.L., Nikoletopoulou, V., Parker, M., Ruzhynsky, V., Alexson, T., McNamara, S.M., Park, D.S., Rudnicki, M. and Slack, R.S. (2004) p107 regulates neural precursor cells in the mammalian brain. *J. Cell. Biol.*, **166**, 853–863.

62. Julian, L.M., Vandenbosch, R., Pakenham, C.A., Andrusiak, M.G., Nguyen, A.P., McClellan, K.A., Svoboda, D.S., Lagace, D.C., Park, D.S., Leone, G. *et al.* (2013) Opposing regulation of Sox2 by cell-cycle effectors E2f3a and E2f3b in neural stem cells. *Cell Stem Cell*, **12**, 440–452.

63. Pham, J., Cabrera, S.M., Sanchis-Segura, C. and Wood, M.A. (2009) Automated scoring of fear-related behavior using EthoVision software. *J. Neurosci. Methods*, **178**, 323–326.

64. Qin, Z., Zhou, X., Gomez-Smith, M., Pandey, N.R., Lee, K.F., Lagace, D.C., Beique, J.C. and Chen, H.H. (2012) LIM domain only 4 (LMO4) regulates calcium-induced calcium release and synaptic plasticity in the hippocampus. *J. Neurosci.*, **32**, 4271–4283.